Therapeutic targeting of human hepatocyte growth factor with a single neutralizing monoclonal antibody reduces lung tumorigenesis

Laura P. Stabile,[1,5] Mary E. Rothstein,[1] Phouthone Keohavong,[2] Jide Jin,[2] Jinling Yin,[2] Stephanie R. Land,[3,5] Sanja Dacic,[4,5] The Minh Luong,[3] K. Jin Kim,[6] Austin M. Dulak,[1] and Jill M. Siegfried[1,5]

Departments of [1]Pharmacology, [2]Environmental and Occupational Health, [3]Biostatistics, and [4]Pathology and [5]Lung and Thoracic Malignancy Program, University of Pittsburgh, Pittsburgh, Pennsylvania and [6]Galaxy Biotech, LLC, Mountain View, California

Abstract

The hepatocyte growth factor (HGF)/c-Met signaling pathway is involved in lung tumor growth and progression, and agents that target this pathway have clinical potential for lung cancer treatment. L2G7, a single potent anti-human HGF neutralizing monoclonal antibody, showed profound inhibition of human HGF-induced phosphorylated mitogen-activated protein kinase induction, wound healing, and invasion in lung tumor cells *in vitro*. Transgenic mice that overexpress human HGF in the airways were used to study the therapeutic efficacy of L2G7 for lung cancer prevention. Mice were treated with the tobacco carcinogen, nitrosamine 4-(methylnitrosamino)-1-(3-pyridyl)-1-butanone, over 4 weeks. Beginning at week 3, i.p. treatment with 100 μg L2G7 or isotype-matched antibody control, 5G8, was initiated and continued through week 15. The mean number of tumors per mouse in the L2G7-treated group was significantly lower than in the control group (1.58 versus 3.19; *P* = 0.0005). Proliferative index was decreased by 48% (*P* = 0.013) in tumors from L2G7-treated mice versus 5G8-treated mice, whereas extent of apoptosis was increased in these same tumors by 5-fold (*P* = 0.0013). Phosphorylated mitogen-activated protein kinase expression was also significantly decreased by 84% in tumors from L2G7-treated mice versus 5G8-treated mice (*P* = 0.0003). Tumors that arose in HGF transgenic animals despite L2G7 treatment were more likely to contain mutant K-*ras*, suggesting that targeting the HGF/c-Met pathway may not be as effective if downstream signaling is activated by a K-*ras* mutation. These preclinical results show that blocking the HGF/c-Met interaction with a single monoclonal antibody delivered systemically can have profound inhibitory effects on development of lung tumors. [Mol Cancer Ther 2008;7(7):1913–22]

Received 10/5/07; revised 3/5/08; accepted 4/10/08.

Grant support: NIH grants R01 CA79882 and P50 CA090440 (J.M. Siegfried). L2G7 and 5G8 were kindly provided by Galaxy Biotech.

The costs of publication of this article were defrayed in part by the payment of page charges. This article must therefore be hereby marked *advertisement* in accordance with 18 U.S.C. Section 1734 solely to indicate this fact.

Requests for reprints: Jill M. Siegfried, The Hillman Cancer Center, UPCI Research Pavilion, Suite 2.18, 5117 Centre Avenue, Pittsburgh, PA 15213-1863. Phone: 412-23-7769; Fax: 412-623-7768. E-mail: Siegfriedjm@upmc.edu

doi:10.1158/1535-7163.MCT-07-2169

Introduction

Lung cancer is the leading cause of cancer death in the United States and the 5-year survival rate is only 16% (1). Lung cancer patients have few therapeutic options; therefore, new targeted strategies are essential to make an effect on this disease. The hepatocyte growth factor (HGF)/c-Met signaling pathway plays a key role in the development and progression of many human cancers, including lung cancer, and represents an attractive targeted pathway for therapeutic intervention (2).

c-Met is a receptor tyrosine kinase and is the only known receptor for HGF, also known as scatter factor (3, 4). Under normal physiologic conditions, the HGF/c-Met pathway plays a role in development and wound healing and is not required for normal tissue homeostasis in the adult. Thus, few adverse effects may result from therapy targeting this pathway. In many types of human cancer, including lung, HGF and/or c-Met is commonly overexpressed compared with normal tissue (5, 6). Furthermore, this correlation has been associated with disease state and clinical outcome (7). An important property of HGF is the ability to induce cell movement. Increased HGF levels within the tumor at time of resection may be an indicator of prior occult migration of malignant cells to other sites, thus increasing the probability of disease recurrence. A correlation between poor outcome and c-Met overexpression has also been observed (8) as well as with coexpression of both c-Met and HGF in lung tumors (9, 10). Other well-characterized biological effects induced by HGF including proliferation, invasion, angiogenesis, and antiapoptotic activity may also explain why overexpression of this pathway could lead to enhanced tumor development and progression. The HGF/c-Met pathway is a point of convergence for heterogeneous interacting signaling networks; thus, a drug targeting this pathway could interfere with many different tumorigenic pathways to increase clinical benefit.

HGF has a unique structure composed of an α-chain containing the NH_2-terminal domain and four kringle domains covalently disulfide linked to a serine protease like β-chain. Kim et al. and Burgess et al. have

independently developed single potent neutralizing anti-HGF monoclonal antibodies (mAb) that can inhibit the various HGF-induced biological activities attributable to both α and β subunits *in vitro* (11, 12). These antibodies have been shown to be highly specific to human HGF with no cross-reactivity to mouse HGF. Using human glioblastoma xenograft models, which express both HGF and c-Met in an autocrine manner, both antibodies were able to inhibit tumor growth and regression in nude mice. Additionally, histologic analysis revealed that tumors from animals treated with the HGF mAb, L2G7, showed decreased cell proliferation and blood vessel area with increased apoptosis (11).

HGF/c-Met signaling in the lung is primarily through a paracrine mechanism whereby the tumors do not express HGF but rather the surrounding stromal tissue expresses and secretes HGF, which then acts on neighboring tumor cells expressing the c-Met receptor (13). This paracrine action of HGF in the lung renders testing these novel HGF mAbs difficult in conventional lung tumor xenografts, because murine HGF produced by the tumor stroma will be unaffected. We recently described a novel transgenic mouse model that overexpresses human HGF in the airways under control of the Clara cell secretory protein promoter and showed that these mice express significantly higher HGF levels in the airway luminal space and have a significantly increased susceptibility to carcinogen-induced lung adenocarcinoma (14). These mice develop lung tumors that mimic aggressive human lung adenocarcinoma with high HGF levels. This model provides a powerful preclinical system to evaluate antitumor agents that target the HGF/c-Met pathway, specifically agents developed against human HGF.

We used this animal model to test the therapeutic potential of anti-human HGF antibody, L2G7. The HGF transgenic mouse model is unique for studying effects of an anti-human HGF neutralizing antibody, because the HGF being overexpressed is human and there is little evidence of murine HGF in the lungs of these animals. We show for the first time that the L2G7 neutralizing human HGF antibody can significantly decrease carcinogen-induced lung carcinogenesis in human HGF transgenic mice and inhibit downstream cancer-related signaling pathways within the tumors. The L2G7 single antibody may have potential as a therapeutic agent in non-small cell lung cancer (NSCLC).

Materials and Methods

Reagents

L2G7 anti-HGF mAb and 5G8 isotype control were obtained under a Material Transfer Agreement with Galaxy Biotech. Nitrosamine 4-(methylnitrosamino)-1-(3-pyridyl)-1-butanone (NNK) was from Toronto Research Chemicals. Recombinant human and mouse HGF (rhHGF or rmHGF, respectively) was purchased from R&D Systems. NSCLC cell line, 201T, was established in our laboratory from primary tissue specimen as described previously (15). These cells do not harbor a K-*ras* mutation (16).

Protein Extraction and Western Analysis

Cells were grown to 75% confluency in T75 flasks. Cells were serum deprived for 48 h followed by addition of rhHGF or rmHGF (10 ng/mL), recombinant human epidermal growth factor (EGF; 10 ng/mL), L2G7 (0-300 ng/mL), or 5G8 (0-300 ng/mL) to the cells and protein was harvested at 10 min after HGF or EGF addition to examine phosphorylated mitogen-activated protein kinase (p-MAPK) expression. Cells were washed one time with ice-cold PBS. Protein was extracted by adding 300 μL ice-cold radioimmunoprecipitation assay buffer (1× PBS, 1% NP-40, 0.5% sodium deoxycholate, 0.1% SDS containing 1 protease inhibitor cocktail/10 mL buffer; Roche Diagnostics). Protein concentration in the supernatant was measured using the BCA-200 Protein Assay Kit (Pierce).

Equal amounts of protein (25 μg) were loaded on a 10% Tricine-SDS gel for phosphorylated p44/p42 MAPK detection. Protein was transferred to nitrocellulose membrane followed by blocking with 5% milk, 1× TBS-Tween 20. Primary antibody was a 1:1,000 dilution of p-MAPK (Cell Signaling Technology) in 5% milk, 1× TBS-Tween 20 at 4°C overnight. Secondary antibody was horseradish peroxidase–conjugated IgG at a 1:2,000 dilution. West Pico chemiluminescent detection was used followed by autoradiography. Immunoreactive bands were quantitated by densitometry and ImageQuant analysis. Blots were stripped and reprobed with actin antibody (Chemicon/Millipore), at a 1:10,000 dilution. Separate gels were run for total MAPK detection using primary antibody at a 1:1,000 dilution (Cell Signaling Technology) and secondary antibody at a 1:2,000 dilution.

Cell Wound-Healing Assay

For wound-healing assays, cells were grown to confluency in six-well plates. Cells were serum starved for 24 h, wounded with a pipette tip, and treated with HGF (10 ng/mL) alone or in combination with L2G7 (300 ng/mL) or 5G8 (300 ng/mL). Cells were examined by light microscopy before the addition of experimental treatments (0 h) and at 72 h after treatment. The wound width was measured at each time point and the percent closure at 72 versus 0 h was calculated. Three wells per experimental treatment and three wounds per well were examined. Results reported are mean ± SE.

Invasion Assay

In vitro invasion assays were carried out in Matrigel-coated Transwell chambers (BD Biosciences). Briefly, serum-deprived 201T NSCLC cells (1×10^4 per well) were plated in a 24-well Biocoat Matrigel Transwell chamber. HGF (10 ng/mL) was added to the medium in the lower chamber as indicated in the figure. L2G7 (300 ng/mL) or 5G8 (300 ng/mL) was added the top and lower chambers as indicated. Cells were incubated at 37°C with 5% CO_2 for 48 h. Cells that invaded the Transwell chamber were fixed and stained using the Diff-Quik staining solutions according to the manufacturer's instructions (VWR International). The membranes were placed on microscope slides and the number of invading cells was scored on a microscope by counting five fields per

membrane under ×40 magnification. Results reported are the mean ± SE.

Mouse Model

All mice used for experiments were HGF transgenic (FVB/N strain) and heterozygous for the transgene with high copy number. Only HGF transgenic mice were used because they carry the human HGF transgene. Wild-type mice produce only murine HGF, which is not inhibited by L2G7. Breeding and identification of transgenic mice were as described previously (14). Equal numbers of males and females were in each experimental group. Mice were given a total of eight i.p. injections of 3 mg NNK (15 μg/μL) over 4 weeks. Beginning at week 3, i.p. treatment with 100 μg L2G7 or isotype-matched antibody control, 5G8, was initiated and continued through week 15. At week 15, all animals were sacrificed and the lungs were inflated with 10% buffered formalin under 25 cm intra-alveolar pressure and removed. Tumors were counted under a dissecting microscope and tumor size was measured using Motic Images 2000 software. Animal care was in strict compliance with the institutional guidelines established by the University of Pittsburgh.

Immunohistochemistry

Lungs were fixed in 10% buffered formalin. Lung samples were paraffin embedded, sliced, and mounted on slides. Paraffin was removed from the slides with xylenes, and slides were stained according to standard procedures. Primary antibody was anti-phosphorylated p44/p42 MAPK (Cell Signaling Technology) or anti-Ki-67 (DakoCytomation) at a 1:100 dilution. The secondary antibody was a biotinylated IgG specific for the primary antibody. Brown staining was considered positive. Negative control staining was done without the addition of primary antibody. For p-MAPK and Ki-67 quantitation, tumors from five tumors or preneoplastic lesions per experimental treatment were read and scored for the number of positive cells per five high-power fields. Results are reported as mean ± SE.

For the apoptosis assay, the number of apoptotic cells was determined using the ApopTag Peroxidase *In situ* Apoptosis Detection Kit (Intergen). Sections were deparafinized as above, incubated with proteinase K for 15 min, and washed two times with water. Slides were incubated in 3% H_2O_2 in PBS for 5 min at room temperature and washed two times with PBS. The slides were then incubated for 15 min at 37°C with a terminal transferase enzyme that catalyzes the addition of digoxigenin-labeled nucleotides to the 3′-OH ends of the fragmented DNA. After color development and counterstain, the specimens were mounted. Slides were read and scored for the number of positive cells in either tumor or preneoplastic lesions per five high-power fields. Results are reported as mean ± SE.

Laser Capture Microdissection of Tumors and K-*ras* Mutation Analysis

For isolation of tumors from the lung, 5-μm tissue sections were prepared from each paraffin-embedded lung tissue block. Each tissue section was transferred to a membrane slide, stained with H&E, and examined by an experienced pathologist to identify and histologically analyze each tumor. Once identified, the areas of interest were taken from the membrane slide by using a fluorescent laser capture microdissection Leica microscope (Application Solution Laser MicroDissection). On the laser action, the dissected area was dropped into the cap of the microcentrifuge tube containing cell lysis buffer and DNA was extracted by proteinase digestion followed by phenol-chloroform extraction and ethanol precipitation. The DNA was dissolved in 10 mmol/L Tris-HCl (pH 8.5), 1 mmol/L EDTA and stored at -20°C until use.

K-*ras* mutations were analyzed as described previously (17) by using the combination of nested PCR to amplify K-*ras* exon 1 that contains codon 12/13 and denaturing gradient gel electrophoresis to separate mutant from wild-type alleles. Experimentally, for the first-round PCR, an aliquot containing an equivalent of 20 to 50 cells was taken from each DNA sample and used for PCR amplification in a final 25 μL volume containing 10 mmol/L Tris-HCl (pH 8.3), 1.5 mmol/L $MgCl_2$, 50 mmol/L KCl, 100 μmol/L each deoxynucleotide triphosphate, 0.3 μmol/L each of the pair of primers (sense 5′-GACATGTTCTAATTTAGTTG-3′ and antisense 5′-AGGCGCTCTTGCCTACGGCA-3′), and 1.0 unit AmpliTaq Gold DNA polymerase (Applied Biosystems). The mixture was heated at 95°C for 9 min and then subjected to 40 cycles (94°C for 1 min, 53°C for 1 min, and 72°C for 1 min). For the second-round PCR, 1 μL of each of the first-round PCR products was then diluted into a final 25 μL reaction mixture containing the same buffer composition as above, except that 0.25 μL [α-^{32}P]dATP (3,000 Ci/mmol; Perkin-Elmer) was added and that primers (antisense) 5′-AGGCGCTCTTGCCTACGGCA-3′ and (sense) 5′-GCCGCCTGCAGCCCGCGCCCCCCGTGCCCCCGCCCCGCCGCCGGCCCGGCGCCCTATTGTAAGGCCTGCTGAAAAT-3′ were used to amplify exon 1. Each reaction mixture was heated at 95°C for 9 min and subjected to 25 PCR cycles (94°C for 1 min, 60°C for 1 min, and 72°C for 1 min). The resulting PCR products were separated by gel electrophoresis and autoradiographed. Bands containing the expected 126-bp exon 1 fragment were excised from the gel. DNA was eluted and analyzed by denaturing gradient gel electrophoresis (Bio-Rad) under the conditions described previously (17) and mutant alleles were further characterized by sequencing.

Statistical Analysis

The number of tumors per group in the NNK carcinogenesis animal study was compared with Poisson regression. The tumor sizes per group (after log transformation) were compared with linear mixed-effects models fitted by the maximum likelihood method. Data from two experiments were combined, and the analysis was adjusted for sex. Significance tests were done with two-sided significance level 0.05. Tukey one-way ANOVA with post-test was used for analysis in Fig. 2. For immunohistochemical analysis in Figs. 4 and 5, an unpaired Student's *t* test was used. For K-*ras* mutation analysis in Table 1, a Fisher's exact test was used.

Results

L2G7 Specifically Inhibits HGF-Induced Biological Activities *In vitro*

We first examined the effect of L2G7 on biological activities of HGF on a lung cancer cell line *in vitro*. We chose the 201T lung adenocarcinoma cell line for these assays because it has been shown to overexpress c-Met and respond to HGF, and we documented previously that these cells do not secrete HGF (18, 19). We first examined the inhibition of HGF-induced p-MAPK in response to increasing concentrations of L2G7. p-MAPK is downstream of c-Met activation, and MAPK induction has been shown to be a highly consistent indicator of HGF activity (19). 201T lung adenocarcinoma cells were treated with L2G7 (0-300 ng/mL) and rhHGF (10 ng/mL). rhHGF induced p-MAPK expression by 6-fold compared with control. L2G7 decreased the rhHGF-induced p-MAPK expression in a concentration-dependent manner (Fig. 1A). A maximum decrease of 76% was observed for p-MAPK expression using 300 ng/mL L2G7. No additional benefit was observed with up to 500 ng/mL L2G7 (data not shown). These experiments were repeated three times with similar results. L2G7 also inhibited HGF-induced phosphorylated c-Met to a similar extent *in vitro*.

We next showed that L2G7 was specific to inhibition of human HGF-induced biological activities. In this regard, recombinant human EGF (10 ng/mL) stimulated p-MAPK by ~7-fold over control and L2G7 (up to 300 ng/mL) showed no ability to inhibit recombinant human EGF-induced p-MAPK (Fig. 1B). Similarly, L2G7 could not block murine HGF; rmHGF-induced p-MAPK expression was unaffected in the presence of L2G7 (Fig. 1C) consistent with previous results (12). L2G7 alone had no effect on basal p-MAPK, and the isotype-matched control antibody, 5G8, also had no effect either in the presence or absence of HGF (Fig. 1A and D).

We next analyzed the effect of the neutralizing antibody on HGF-induced wound healing (Fig. 2A and B). Serum-starved 201T cells were treated with or without 10 ng/mL HGF in the presence or absence of 300 ng/mL L2G7 or 5G8. HGF treatment alone was able to close a pipette generated wound 80.53% compared with the no treatment wound closure of only 1.67% after 72 h ($P < 0.001$). The percent wound closure in the presence of L2G7 and HGF was only 13.67% (>80% inhibition of HGF-induced wound healing; $P < 0.001$, HGF versus L2G7 + HGF), whereas 5G8 plus HGF wound closure was not significantly different from HGF treatment alone wound closure ($P > 0.05$, HGF versus 5G8 + HGF). L2G7 or 5G8 alone had no significant effect on wound healing and was similar to control untreated cells.

Another well-documented biological activity of HGF is cell invasion. We used movement through an artificial extracellular Matrigel matrix as a measure of relative invasion of 201T cells to assess whether L2G7 could inhibit HGF-induced invasion (Fig. 2C). HGF induced invasion by 1.3-fold in this assay ($P < 0.001$). This stimulation was inhibited below basal levels in the presence of L2G7 treatment ($P < 0.001$, HGF versus HGF + L2G7). 5G8 in the presence of HGF had no effect on HGF-induced cell invasion ($P > 0.05$, HGF versus 5G8 + HGF). L2G7 or 5G8 alone had no significant effect on invasion and were similar to control untreated cells. Similar effects of L2G7 were observed on HGF-induced cell proliferation (data not shown). Thus, several distinct biological responses to HGF were found to be specifically inhibited by L2G7 in human lung tumor cells *in vitro*. This established a rationale to test L2G7 in an *in vivo* preclinical model.

Inhibition of Lung Tumor Formation by L2G7 Treatment

We used a transgenic mouse model that overexpresses human HGF in the airways to test the efficacy of L2G7 in an *in vivo* model of lung adenocarcinoma tumorigenesis. We documented previously that these animals express high levels of human HGF in the lungs (14). Because the L2G7 antibody does not recognize murine HGF, this transgenic mouse is a unique system to study this mAb *in vivo* against lung tumors that normally show only paracrine HGF secretion. All mice were treated with a tobacco carcinogen, NNK, for 2 weeks before the initiation of L2G7 HGF mAb or 5G8 control treatment. mAb treatment (100 μg/injection) continued until week 15 when the animals were sacrificed. We chose this time point to begin L2G7 treatment to mimic the human setting whereby there is exposure to tobacco before chemopreventative measures. In addition, the effect of HGF is more likely to inhibit the promotion phase of tumor cell growth and progression than to inhibit the initiation phase of mutation and establishment of preneoplastic lesions.

The results from two separate experiments were combined for this analysis.

The 5G8 control group consisted of 24 mice in total, whereas the L2G7 treatment group included 22 mice. Seven of the 22 mice (31.8%) in the L2G7-treated arm did not develop any visible lung tumors, whereas only 4 of the 24 (16.7%) in the 5G8 arm did not develop visible tumors. The mean number of tumors per mouse in the group treated with L2G7 was significantly lower than in the 5G8 control group ($P < 0.001$). The estimated geometric mean, adjusted for sex, of the number of tumors per mouse in the group treated with L2G7 was 1.58 (median, 1; range, 0-6), whereas in the control group it was 3.19 (median, 3.5; range, 0-7; Fig. 3A).

There was not a significant difference in tumor size ($P = 0.974$) between L2G7- and 5G8-treated groups. There was one very large outlier (in the 5G8 group) and there was

Table 1. K-*ras* mutations in tumors from L2G7- and 5G8-treated mice

K-ras status	L2G7, *n* (%)	5G8, *n* (%)
G12D	25 (73.5)	12 (44.4)
Wild-type	9 (26.5)	15 (55.6)
Total	34 (100)	27 (100)

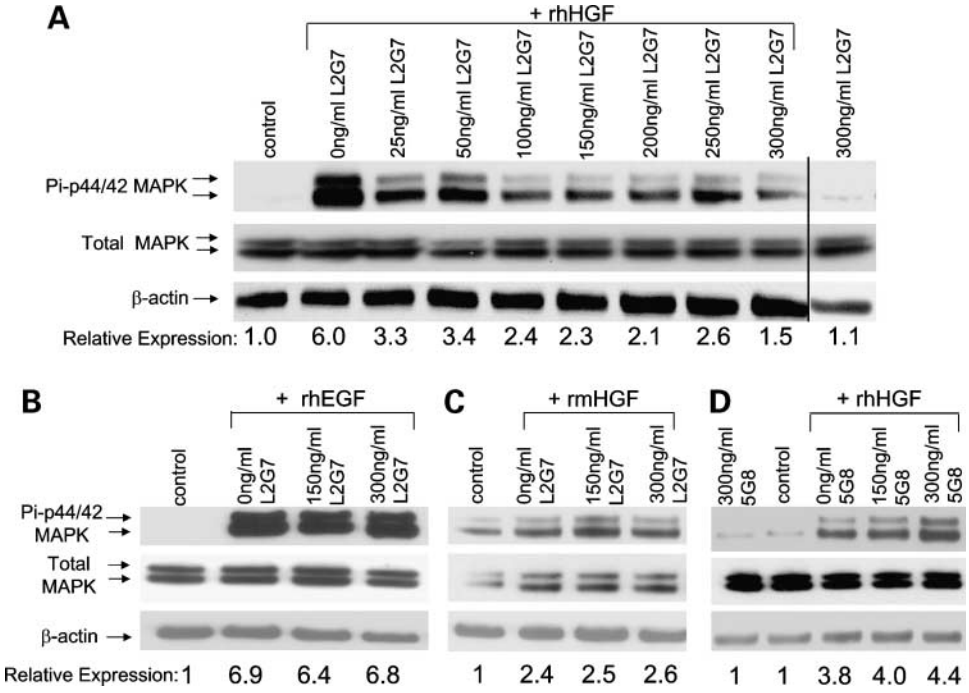

Figure 1. L2G7 inhibits human HGF-induced p-MAPK expression. **A,** 201T cells were serum deprived for 48 h followed by treatment with 0 to 300 ng/mL L2G7 and the addition of (**A**) 10 ng/mL rhHGF, (**B**) 10 ng/mL recombinant human EGF, or (**C**) 10 ng/mL rmHGF for 10 min. Cell lysates were prepared and analyzed for p-MAPK expression. The blots were stripped and reprobed for β-actin. Relative quantitation is shown beneath each blot. Separate gels were run for total MAPK expression. **D,** 201T cells were cultured as described above. Following serum deprivation, cells were treated with 5G8 control antibody (0-300 ng/mL) in the presence or absence of rhHGF (10 ng/mL). p-MAPK, total MAPK, and β-actin expression were analyzed as in **A** to **C**.

substantial overlap in the data. The median tumor size in the L2G7-treated group was 0.33 mm^2 (interquartile range, 0.22-0.45 mm^2; range, 0.12-2.44 mm^2), and the median size in the 5G8 group also was 0.33 mm^2 (interquartile range, 0.21-0.55 mm^2; range, 0.10-5.50 mm^2). Figure 3B shows a histogram of the frequency of tumor sizes by treatment group. Although there was no difference in median tumor size among treatment groups, there were fewer larger tumors found in the L2G7 treatment group compared with the 5G8 treatment group based on the distribution frequency. For example, 5 of 36 (13.8%) tumors from the L2G7-treated group were in the $\geq$0.7 mm^2 size category, whereas 16 of 78 (21%) tumors fell in this category from the 5G8-treated group.

In the multistep carcinogenesis model for lung cancer (20), peripheral adenocarcinoma of the lung develops from noninvasive precursor lesions known as atypical adenomatous hyperplasia. No significant difference was observed in the number of adenomatous lesions or bronchiolar hyperplasia present after 13 weeks of therapy between mice treated with L2G7 and mice treated with 5G8 (data not shown), suggesting that L2G7 does not block early carcinogenic events but more likely affects tumor cell turnover, doubling time, or progression. In addition, in an alternate protocol in which the antibody treatment was initiated 1 week before NNK treatment and then continued for an additional 15 weeks, we observed no additional benefit of L2G7 compared with initiating L2G7 treatment during NNK treatment (data not shown). In both protocols, L2G7 treatment reduced tumorigenicity to about half the level observed with control antibody. In previous experiments comparing wild-type littermates with HGF transgenic mice, we also observed about half as many lung tumors in wild-type animals as in carriers of the transgene (14), suggesting that L2G7 treatment almost completely inhibited the ability of the human HGF transgene to increase susceptibility to lung cancer.

Signaling in Tumors and Preneoplastic Lesions Is Affected by L2G7 Treatment

We next examined lung tumors removed from mice treated with L2G7 or 5G8 and analyzed the number of proliferating cells by Ki-67 immunohistochemistry. The number of Ki-67-positive cells in tumors from L2G7-treated mice was 48% lower than that found in tumors from 5G8-treated mice ($P < 0.05$; Fig. 4A). Additionally, because MAPK is a signaling pathway known to be induced by HGF and we have shown in Fig. 1A that L2G7 can inhibit this signaling pathway *in vitro*, we examined whether L2G7 reduced the number of p-MAPK-positive cells found in HGF-overexpressing tumors (Fig. 4B). Tumors from L2G7-treated animals showed 84% fewer p-MAPK-positive cells compared with tumors examined from 5G8-treated mice ($P < 0.0005$). In contrast, the number of apoptotic cells as examined using a terminal deoxynucleotidyl transferase–mediated dUTP nick end labeling assay was significantly increased by 5-fold in tumors from L2G7-treated animals compared with tumors from 5G8-treated animals ($P < 0.005$; Fig. 4C).

Similar effects on expression of signaling molecules were observed in adenomatous hyperplasia lesions of the lung. In this regard, a 34% and 41% decrease was observed in adenomatous hyperplasia lesions of similar size from L2G7-treated animals versus 5G8-treated animals for Ki-67 and p-MAPK expression, respectively ($P < 0.05$ and $P = 0.06$; Fig. 5A and B). In addition, the number of apoptotic cells was increased 3.2-fold ($P < 0.005$) in

adenomatous hyperplasia lesions of similar size from L2G7-treated animals compared with 5G8-treated animals (Fig. 5C). These findings suggest that although the number of preneoplastic lesions was not reduced by L2G7 treatment, the ratio of proliferative to apoptotic signals within these lesions was lowered by the HGF neutralizing antibody.

Tumors with K-*ras* Mutation Are Resistant to L2G7 Treatment

Activation of the K-*ras* proto-oncogene through mutations is a common event in lung cancer, especially in murine adenocarcinomas induced to NNK, and we examined whether L2G7 treatment could inhibit tumors harboring a K-*ras* activating mutation. Laser capture microdissection was used to isolate tumors from tissue sections for subsequent genomic DNA extraction and K-*ras* mutation analysis in codons 12 and 13. Greater than 95% of ras mutations are found in these codons (21). All activating mutations switch Ras to its GTP-bound, constitutively active state. Thirty-four tumors were isolated from the L2G7-treated group and 27 tumors from the 5G8-treated group. Some tumors had already been depleted from the previous assays; thus, the entire dataset could not be analyzed. Table 1 shows that in the presence of L2G7, which produces ~50% inhibition of tumorigenesis, tumors that did form were more likely to be K-*ras* mutant. K-*ras* mutations were found in 73.5% (25 of 34) of tumors from L2G7-treated animals and 44.4% (12 of 27) of tumors from 5G8-treated animals (P = 0.034, Fisher's exact test). All K-*ras* mutations found were located in codon 12 and corresponded to a GGT-to-GAT transition of glycine to aspartate (G12D). K-*ras* mutation status in FVB/N wild-type littermates exposed to NNK showed a 40% incidence rate of K-*ras* mutations (data not shown), similar to that observed in HGF transgenic animals treated with 5G8. This suggests that the HGF transgene in general promotes both K-*ras* mutant and wild-type tumors but that K-*ras* mutant tumors are less responsive to withdrawal of HGF signaling. These results suggest that targeting the HGF/c-Met pathway in patients may not be as effective if tumors contain activating K-*ras* mutations. We did, however, note that Ki-67 and apoptotic cell labeling showed equal alterations from L2G7 treatment in some tumors that formed which had K-*ras* activating mutations or K-*ras* wild-type status (data not shown).

To further examine the effects of HGF signaling withdrawal in lung tumor cells that express c-Met and contain a K-*ras* mutation, MAPK phosphorylation was measured at baseline and following HGF stimulation in three NSCLC cell lines containing K-*ras* point mutations (16, 17). In 343T cells containing the K-*ras* mutation G12C, basal p-MAPK was highly expressed, no increase in p-MAPK was observed with HGF, and there was no appreciable decrease in p-MAPK with L2G7 (Supplementary Fig. S1A).[7] In 91T cells containing the G12V K-*ras* mutation, basal p-MAPK was low, there was a strong 8-fold

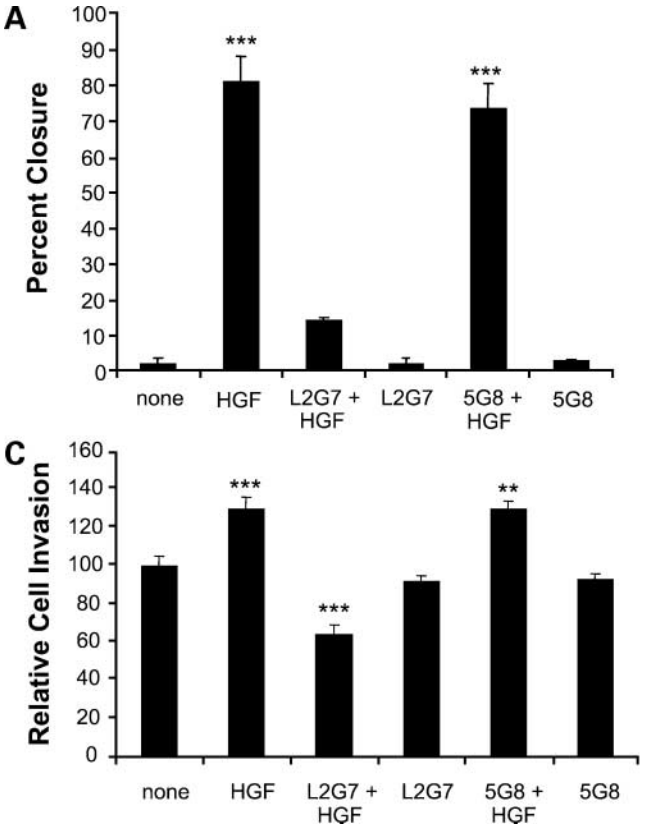

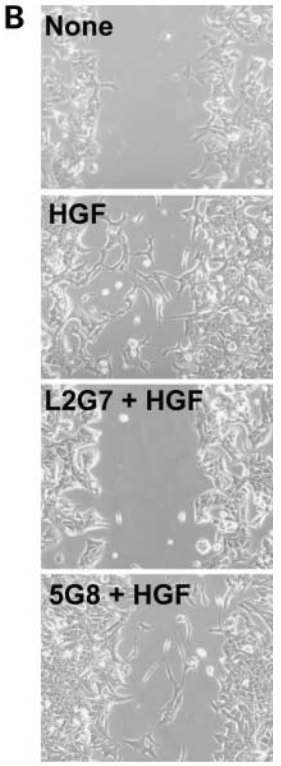

Figure 2. L2G7 blocks HGF-induced wound healing and cell invasion. **A,** 201T cells were serum deprived followed by treatment with HGF (10 ng/mL), L2G7 (300 ng/mL), or 5G8 (300 ng/mL) as indicated for 72 h. Wound-healing assays were done and the mean of six samples per treatment group is expressed compared with control, untreated wells. *Bars,* SE. ***, $P < 0.001$, ANOVA. **B,** representative photographs of cells at 72 h following experimental treatments as indicated. **C,** 201T cells were serum deprived before plating in invasion chamber wells. Cells were treated with HGF (10 ng/mL), L2G7 (300 ng/mL), or 5G8 (300 ng/mL) as indicated in the figure. Forty-eight hours following treatment, invading cells were fixed and stained. Positively stained cells in five high-power fields per slide were counted at ×40 magnification. Mean of four samples per treatment group; *bars,* SE. **, $P < 0.01$; ***, $P < 0.001$, ANOVA. All comparisons were respective to control untreated cells.

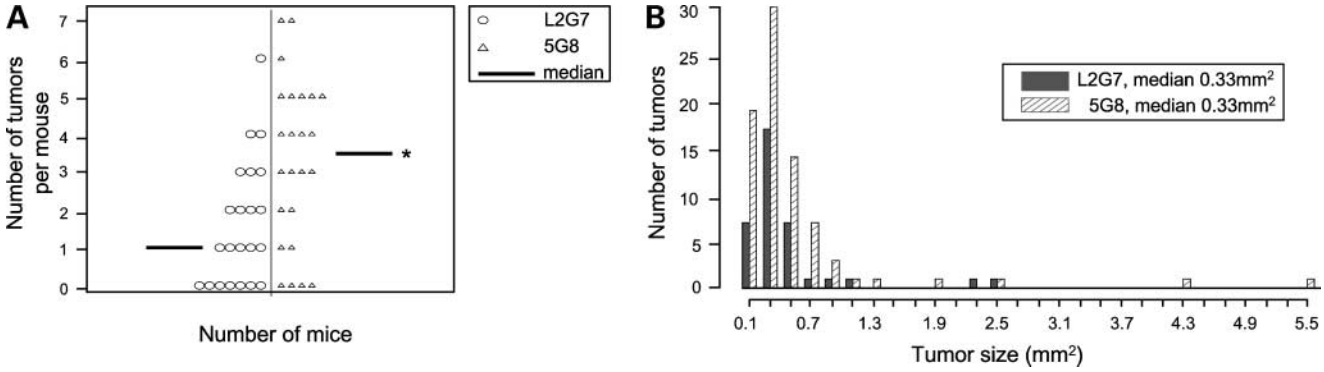

Figure 3. Tumor formation following NNK exposure in HGF transgenic mice treated with L2G7 neutralizing antibody to human HGF or control 5G8 isotype-matched antibody. **A,** number of tumors per mouse by treatment group for the combined data set. Each point in the figure represents one mouse (*circle,* L2G7-treated mouse; *triangle,* 5G8-treated mouse). *Horizontal line within each side,* median for the treatment group. *, $P < 0.001$. **B,** histogram of tumor sizes (mm^2) by treatment group for combined data set. Intergroup differences: $P = 0.752$.

increase with HGF, but the neutralizing antibody L2G7 was much less effective (maximum inhibition 38%; Supplementary Fig. S1B).[7] A similar result was observed with A549 cells, K-*ras* mutation G12S (data not shown). Dependence on HGF signaling or an ability to inhibit HGF signaling may be reduced in NSCLC cell lines with K-*ras* mutation compared with wild-type K-*ras* cells, such as 201T (Fig. 1).

Discussion

Because of the overwhelming evidence for the role of the HGF/c-Met pathway in the pathogenesis of human cancers, therapeutic inhibitors that target this pathway are being developed for clinical use. mAbs and small-molecule tyrosine kinase inhibitors represent the most feasible approaches and are the most clinically relevant agents at this time. Currently, there are phase I clinical trials for cancer therapy in progress for both of these classes of drugs. This pathway may be desirable for cancer therapeutic inhibition because side effects associated with inhibition of this pathway in the absence of wound healing would potentially be low.

We have shown here that a human HGF mAb, L2G7, can profoundly inhibit HGF-induced activation of MAPK as well as biological responses in NSCLC *in vitro* (wound healing and cell invasion). L2G7 was inactive against either EGF or recombinant murine HGF, thus showing specificity for human HGF. The anti-HGF neutralizing antibody also substantially inhibited tumor formation in transgenic mice overexpressing the human HGF gene in the airways; there was ~2-fold difference between tumor formation with the control antibody treatment and tumor formation with the neutralizing antibody. This is the same order of magnitude as the observed 2-fold difference in lung tumor formation between HGF transgenic and wild-type mice (14), suggesting that almost all the biological effect of the human HGF transgene was abolished by L2G7. L2G7 treatment also significantly altered critical signaling pathways within the tumors. In this regard, proliferation index as measured by Ki-67 immunostaining was significantly decreased as well as p-MAPK expression, a well-established signaling pathway involved in lung tumor cell growth. The HGF signaling pathway also shows antiapoptotic effects (22). Treatment with L2G7 blocked this function as well. These effects were observed in tumors and to a lesser extent in hyperplastic lesions of the lung. The inhibition of signaling occurred in both K-*ras* wild-type tumors and K-*ras* mutant tumors. Therefore, although L2G7 appears to have less overall effect on reducing formation of K-*ras* mutant tumors detected by this protocol, downstream signaling is still diminished by L2G7 even in the presence of mutant K-*ras* in this model.

The effect of L2G7 did not appear to be related to tumor initiation but rather to tumor progression because the number of preneoplastic areas in the lungs from L2G7-treated versus 5G8-treated animals was not significantly altered, but the number of adenomas was significantly decreased. Additional evidence for an effect on the promotional phase was seen in that starting the L2G7 treatments before NNK exposure did not exhibit a greater inhibitory effect compared with starting L2G7 treatment during the course of NNK exposure. Median tumor size was not affected by L2G7 treatment; however, the largest tumors were observed in the 5G8 control antibody-treated group. We also compared K-*ras* status versus tumor size in a subset of tumors where both variables were known. No difference in mean or median tumor size between treatment groups was observed when analyzing K-*ras* mutants only or K-*ras* wild-type tumors only, suggesting that both groups have equal ability to proliferate.

Mutations in *ras* genes are found in ~30% of human cancers (23). K-*ras* mutations are the most linked to NSCLC and occurs in 20% to 30% of lung adenocarcinoma (17, 23). Overall, K-*ras* appears to be a weak negative prognostic marker in adenocarcinoma of the lung (24, 25). The major type of K-*ras* mutation that we report in lung tumors is similar to other reports (26, 27). In the studies presented

[7] Supplementary material for this article is available at Molecular Cancer Therapeutics Online (http://mct.aacrjournals.org/).

here, the K-*ras* wild-type tumors are selectively targeted with the L2G7 neutralizing antibody to human HGF, suggesting that downstream constitutive activation of the ras pathway in K-*ras* mutant tumors make them more resistant to inhibition that blocks an upstream tyrosine kinase receptor. We also observed that NSCLC cell lines with K-*ras* mutations either showed high basal p-MAPK with little induction by HGF or HGF signaling could not be effectively inhibited by the neutralizing antibody. When signaling to p-MAPK was HGF dependent in K-*ras* mutants, it is not clear what would cause the resistance to HGF neutralizing antibody. The K-*ras* mutant cells showed similar HGF concentration dependence as K-*ras* wild-type cells. It is possible that the physical association between activated K-*ras* and c-Met compared with wild-type K-*ras* and c-Met has different dynamics in the presence of the HGF neutralizing antibody complex. The exact mechanism warrants further study. Both *in vivo* and *in vitro* observations suggest that effective targeting of c-Met signaling could be accomplished more efficiently when there is not a K-*ras* mutation present. This is similar to inhibition of other receptor tyrosine kinase pathways; there is an apparent negative association between K-*ras* mutations and mutations in the EGF receptor (EGFR) tyrosine kinase domain that determine patient response to EGFR tyrosine kinase inhibitors (16, 28). This may prove to be the case with HGF/c-Met inhibition as well.

c-Met activation is involved in different steps of tumorigenesis including tumor formation, growth, and spreading in many different solid tumor types. In addition, this pathway interacts with several other tumorigenic pathways, including the EGFR signaling pathway, making this pathway an attractive target for therapy. For example, when EGFR is overexpressed in tumor cells, it can directly associate with and phosphorylate c-Met (29). Additionally, amplification of c-Met is a mechanism of resistance to the EGFR tyrosine kinase inhibitor gefitinib (30). With the anticipation that combinations of pathway selective therapies will most likely be necessary for many cancer types, this therapy may also be beneficial for combined therapy with other drugs, particularly with agents that target the EGFR, cyclooxygenase-2, or vascular endothelial growth factor pathways. We have recently shown that HGF can induce cyclooxygenase-2 expression and release prostaglandin E_2, which can then act to directly activate c-Met in lung cancer cells in a HGF-independent manner (19), suggesting that dual targeting of HGF/c-Met with cyclooxygenase-2 may be beneficial. There is also evidence that HGF can induce angiogenesis independently of the vascular endothelial growth factor pathway (31), indicating

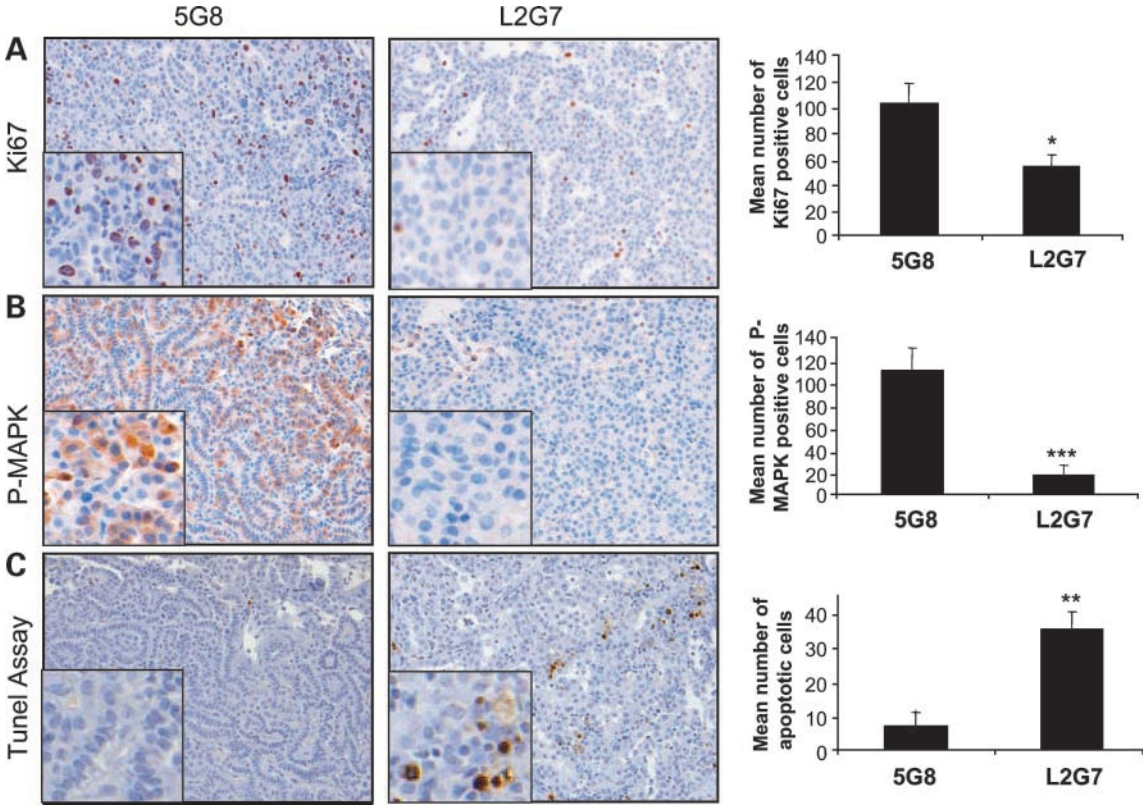

Figure 4. Representative tumor sections from 5G8- and L2G7-treated animals showing immunohistochemical staining for (**A**) Ki-67, (**B**) p-MAPK, and (**C**) apoptotic cells. *Inset,* 2-fold high-power view. Quantitation for each marker was done. Mean ± SE number of positive cells for each marker from five high-power fields from five tumors per experimental treatment. *, $P < 0.05$; **, $P < 0.005$; ***, $P < 0.0005$, Student's *t* test.

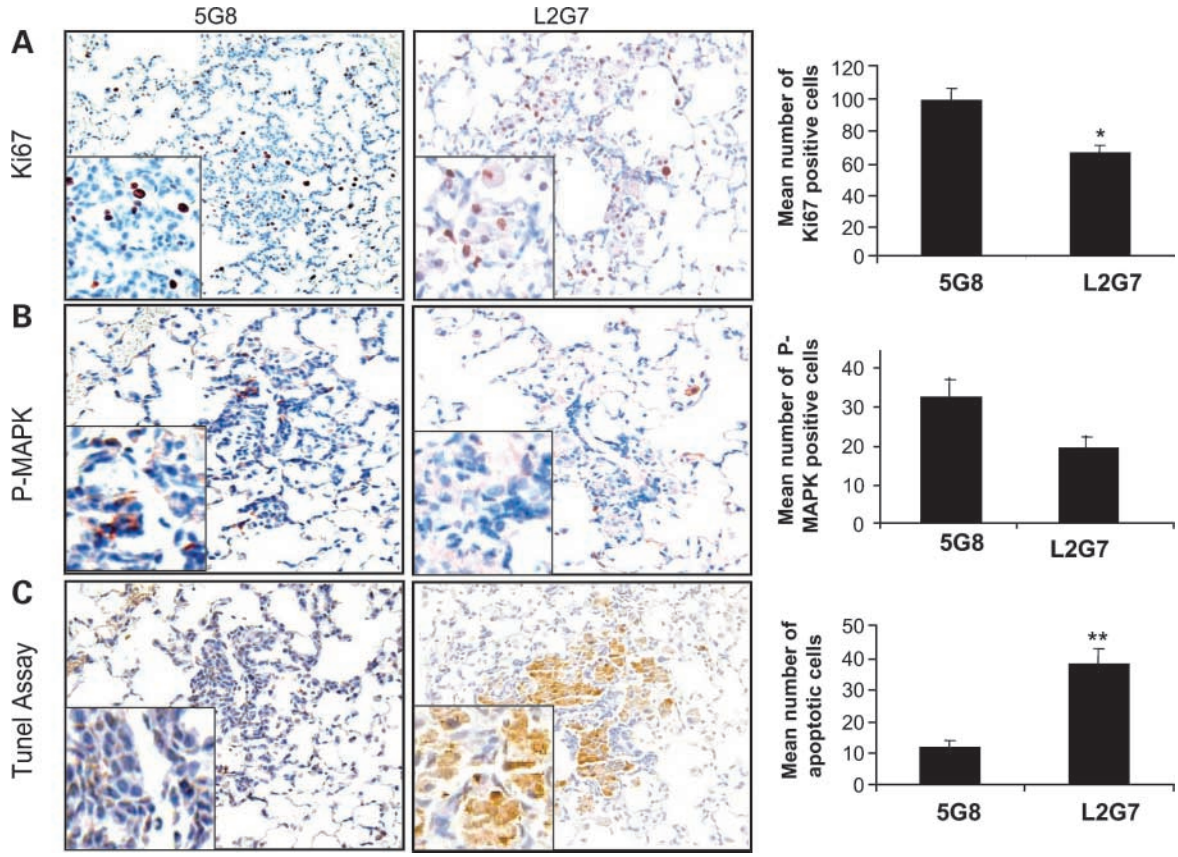

Figure 5. Representative preneoplastic sections from 5G8- and L2G7-treated animals showing immunohistochemical staining for (**A**) Ki-67, (**B**) p-MAPK, and (**C**) apoptotic cells. *Inset,* 2-fold high-power view. Quantitation for each marker was done. Mean ± SE number of positive cells for each marker from five high-power fields from five tumors per experimental treatment. *, $P < 0.05$; **, $P < 0.005$, Student's *t* test.

that inhibition of both HGF and vascular endothelial growth factor pathways may be advantageous as well. The HGF transgenic mouse model used in these studies would be an extremely useful model system to study these types of combination therapies.

In summary, this work shows that therapeutic targeting of the HGF pathway with L2G7 or other agents targeting this pathway has potential to move to human clinical trials for NSCLC. Additionally, K-*ras* mutation status will most likely be a critical part of a panel of markers that will have predictive value for HGF/c-Met targeted therapy. Future challenges will be to accurately identify patients who are most likely to respond to HGF/c-Met targeted therapies, understand the effect of long-term blockade of this pathway, and identify other pathways that would be beneficial to target in combination treatment regimens for enhanced antitumorigenic effects. Understanding these combined issues might enable us to better understand, control, and treat NSCLC.

Disclosure of Potential Conflicts of Interest

K.J. Kim: Galaxy Biotech employee and patent holder. The other authors reported no potential conflicts of interest.

Acknowledgments

We thank Lisa Chedwick (Research Histological Services at the University of Pittsburgh) for technical assistance with the immunohistochemistry experiments.

References

1. American Cancer Society Surveillance Research. Cancer facts and figures 2007. Atlanta (GA): American Cancer Society; 2007. p. 14.

2. Christensen JG, Burrows J, Salgia R. c-Met as a target for human cancer and characterization of inhibitors for therapeutic intervention. Cancer Lett 2005;225:1 – 26.

3. Naldini L, Weidner KM, Vigna E, et al. Scatter factor and hepatocyte growth factor are indistinguishable ligands for the MET receptor. EMBO J 1991;10:2867 – 78.

4. Bottaro DP, Rubin JS, Faletto DL, et al. Identification of the hepatocyte growth factor receptor as the c-met proto-oncogene product. Science 1991;251:802 – 4.

5. Birchmeier C, Birchmeier W, Gherardi E, Vande Woude GF. Met, metastasis, motility and more. Nat Rev Mol Cell Biol 2003;4:915 – 25.

6. Maulik G, Shrikhande A, Kijima T, Ma PC, Morrison PT, Salgia R. Role of the hepatocyte growth factor receptor, c-Met, in oncogenesis and potential for therapeutic inhibition. Cytokine Growth Factor Rev 2002;13: 41 – 59.

7. Siegfried JM, Luketich JD, Stabile LP, Christie N, Land SR. Elevated hepatocyte growth factor level correlates with poor outcome in early-stage and late-stage adenocarcinoma of the lung. Chest 2004;125: S116 – 9.

8. Ichimura E, Maeshima A, Nakajima T, Nakamura T. Expression of c-met/

HGF receptor in human non-small cell lung carcinomas *in vitro* and *in vivo* and its prognostic significance. Jpn J Cancer Res 1996;87:1063 – 9.

9. Harvey P, Warn A, Newman P, Perry LJ, Ball RY, Warn RM. Immunoreactivity for hepatocyte growth factor/scatter factor and its receptor, met, in human lung carcinomas and malignant mesotheliomas. J Pathol 1996;180:389 – 94.

10. Takanami I, Tanana F, Hashizume T, et al. Hepatocyte growth factor and c-Met/hepatocyte growth factor receptor in pulmonary adenocarcinomas: an evaluation of their expression as prognostic markers. Oncology 1996;53:392 – 7.

11. Kim KJ, Wang L, Su YC, et al. Systemic anti-hepatocyte growth factor monoclonal antibody therapy induces the regression of intracranial glioma xenografts. Clin Cancer Res 2006;12:1292 – 8.

12. Burgess T, Coxon A, Meyer S, et al. Fully human monoclonal antibodies to hepatocyte growth factor with therapeutic potential against hepatocyte growth factor/c-Met-dependent human tumors. Cancer Res 2006;66:1721 – 9.

13. Singh-Kaw P, Zarnegar R, Siegfried JM. Stimulatory effects of hepatocyte growth factor on normal and neoplastic human bronchial epithelial cells. Am J Physiol 1995;268:L1012 – 20.

14. Stabile LP, Lyker JS, Land SR, Dacic S, Zamboni BA, Siegfried JM. Transgenic mice overexpressing hepatocyte growth factor in the airways show increased susceptibility to lung cancer. Carcinogenesis 2006;27:1547 – 55.

15. Siegfried JM, Krishnamachary N, Gaither Davis A, Gubish C, Hunt JD, Shriver SP. Evidence for autocrine actions of neuromedin B and gastrin-releasing peptide in non-small cell lung cancer. Pulm Pharmacol Ther 1999;12:291 – 302.

16. Zhang W, Stabile LP, Keohavong P, et al. Mutation and polymorphism in the EGFR-TK domain associated with lung cancer. J Thor Oncol 2006;1:635 – 47.

17. Keohavong P, DeMichele MAA, Melacrinos AC, Landreneau RJ, Weyant RJ, Siegfried JM. Detection of K-ras mutations in lung carcinomas: relationship to prognosis. Clin Cancer Res 1996;2:411 – 8.

18. Stabile LP, Lyker JS, Huang L, Siegfried JM. Inhibition of human non-small cell lung tumors by a c-Met antisense/U6 expression plasmid strategy. Gene Ther 2004;11:325 – 35.

19. Siegfried JM, Gubish CT, Rothstein ME, Queiroz De Oliveira PE, Stabile LP. Signaling pathways involved in cyclooxygenase-2 induction by hepatocyte growth factor in non-small cell lung cancer. Mol Pharmacol 2007;72:769 – 79.

20. Kitamura H, Kameda Y, Ito T, Hayashi H. Atypical adenomatous hyperplasia of the lung. Implications for the pathogenesis of peripheral lung adenocarcinoma. Am J Clin Pathol 1999;111:610 – 22.

21. Molina JR, Adjei AA. The Ras/Raf/MAPK pathway. J Thorac Oncol 2006;1:7 – 9.

22. Kitta K, Day RM, Ikeda T, Suzuki YJ. Hepatocyte growth factor protects cardiac myocytes against oxidative stress-induced apoptosis. Free Radic Biol Med 2001;31:902 – 10.

23. Adjei AA. Blocking oncogenic Ras signaling for cancer therapy. J Natl Cancer Inst 2001;93:1062 – 74.

24. Graziano SL, Gamble GP, Newman NB, et al. Prognostic significance of K-ras codon 12 mutations in patients with resected stage I and II non-small-cell lung cancer. J Clin Oncol 1999;17:668 – 75.

25. Huncharek M, Muscat J, Geschwind JF. K-ras oncogene mutation as a prognostic marker in non-small cell lung cancer: a combined analysis of 881 cases. Carcinogenesis 1999;20:1507 – 10.

26. Ton TV, Hong HH, Anna CH, et al. Predominant K-ras codon 12 G -> A transition in chemically induced lung neoplasms in B6C3F1 mice. Toxicol Pathol 2004;32:16 – 21.

27. Calvert RJ, Buzard GS, Anisimov VN, Rice JM. K-ras codon 12 and 61 point mutations in bromodeoxyuridine- and *N*-nitrosomethylurea-induced rat renal mesenchymal tumors. Cancer Lett 1996;109:1 – 7.

28. Janne PA, Engelman JA, Johnson BE. Epidermal growth factor receptor mutations in non-small-cell lung cancer: implications for treatment and tumor biology. J Clin Oncol 2005;23:3227 – 34.

29. Jo M, Stolz DB, Esplen JE, Dorko K, Michalopoulos GK, Strom SC. Cross-talk between epidermal growth factor receptor and c-Met signal pathways in transformed cells. J Biol Chem 2000;275:8806 – 11.

30. Engelman JA, Zejnullahu K, Mitsudomi T, et al. MET amplification leads to gefitinib resistance in lung cancer by activating ERBB3 signaling. Science 2007;316:1039 – 43.

31. Sengupta S, Gherardi E, Sellers LA, Wood JM, Sasisekharan R, Fan TPD. Hepatocyte growth factor/scatter factor can induce angiogenesis independently of vascular endothelial growth factor. Arterioscler Thromb Vasc Biol 2003;23:69 – 75.

Molecular Cancer Therapeutics

Therapeutic targeting of human hepatocyte growth factor with a single neutralizing monoclonal antibody reduces lung tumorigenesis

Laura P. Stabile, Mary E. Rothstein, Phouthone Keohavong, et al.

Mol Cancer Ther 2008;7:1913-1922.